DOI: 10.1038/ncb3280

nature cell biology

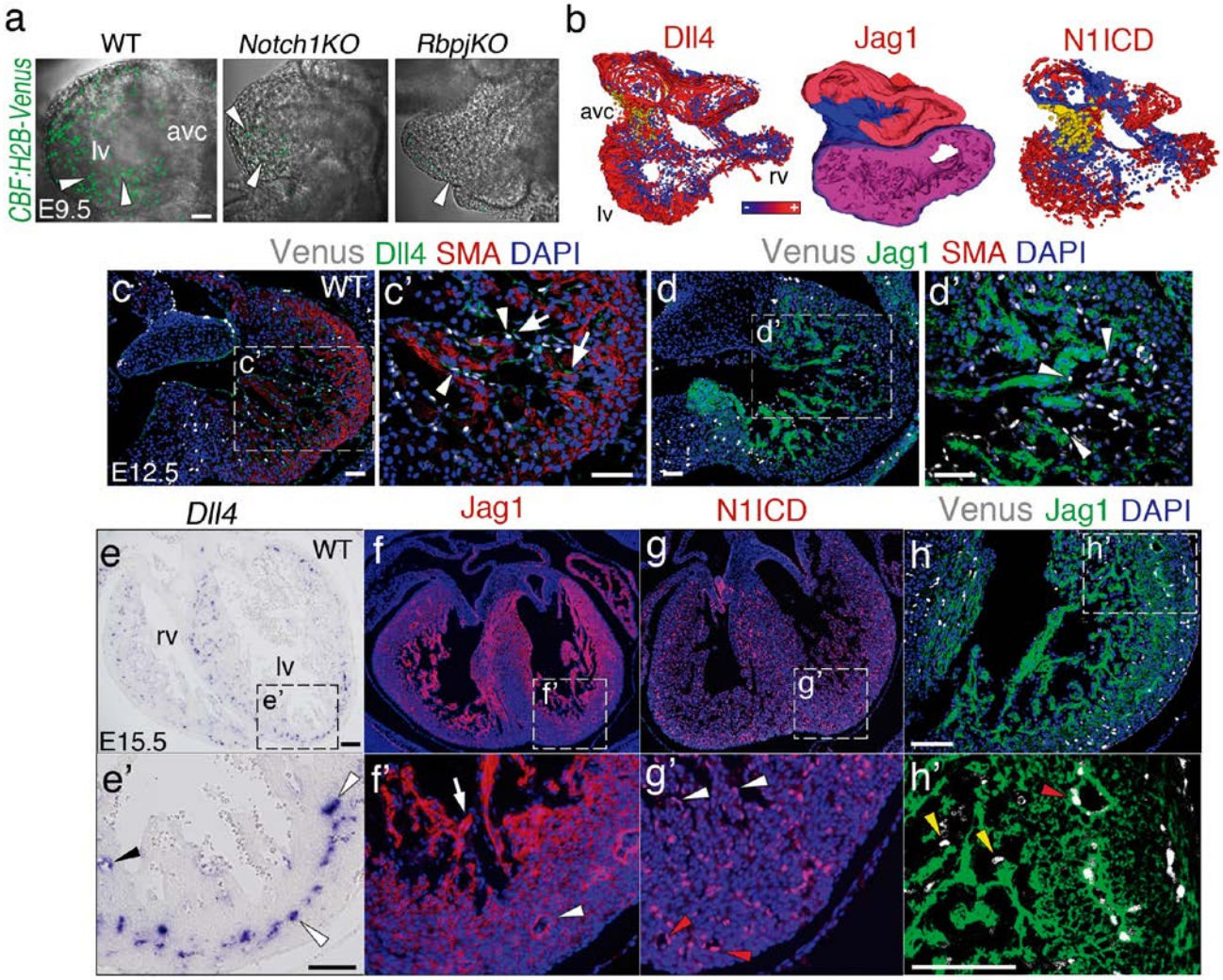

Supplementary Figure 1 *CBF:H2B-Venus* activity in chamber endocardium (**a**) and Dll4 and Jag1 activate Notch during chamber development (**b-h'**). (**a**) Two-photon whole-mount images of the left ventricle of E9.5 *CBF:H2B-Venus*, *CBF:H2B-Venus;Notch1KO* and *CBF:H2B-Venus;RbpjKO* embryos. Arrowheads indicate endocardial Venus expression in WT mice and abrogated expression in *Notch1KO* and *RbpjKO* embryos. (**b**) Images showing rear views of Amira 3D reconstructions of Dll4, Jag1 and N1ICD expression in the E9.5 WT heart. Atrioventricular canal region (avc) mesenchyme (yellow) does not express N1ICD. lv, left ventricle; rv right ventricle. (**c,c'**) Dll4 (green), SMA (red), and Venus (grey) immunostaining in E12.5 WT *CBF:H2B-Venus* ventricles. Venus+ cells (**c'**, arrowheads) distribute throughout the endocardium, similarly to Dll4 (arrows). (**d,d'**) Jag1 (green), SMA (red), and Venus (grey) immunostaining in E12.5 WT *CBF:H2B-Venus* ventricles. In (**c-d'**) nuclei are counterstained with DAPI. Scale bar=50μm. (**e-h'**) E15.5, WT ventricles. (**e,e'**) ISH. *Dll4* is transcribed in coronary vessel endothelium (**e'**, white arrowheads) and some endocardial cells (black arrowhead). (**f-h'**) Immunostainings. (**f,f'**) Jag1 is expressed in trabecular myocardium (**f'**, arrow), and coronary vessels (**f'**, arrowhead). (**g,g'**) N1ICD is expressed in trabecular endocardium (**g'**, white arrowheads) and coronary vessels endothelium (**g'**, red arrowhead). (**h,h'**) Jag1 (green) and Venus (grey) expression in a *CBF:H2B-Venus* reporter embryo. Endocardial cells (yellow arrowheads) and coronary vessel endothelium (red arrowheads) are Venus+. Scale bar=100μm. Source data available in Supplementary Table 4.

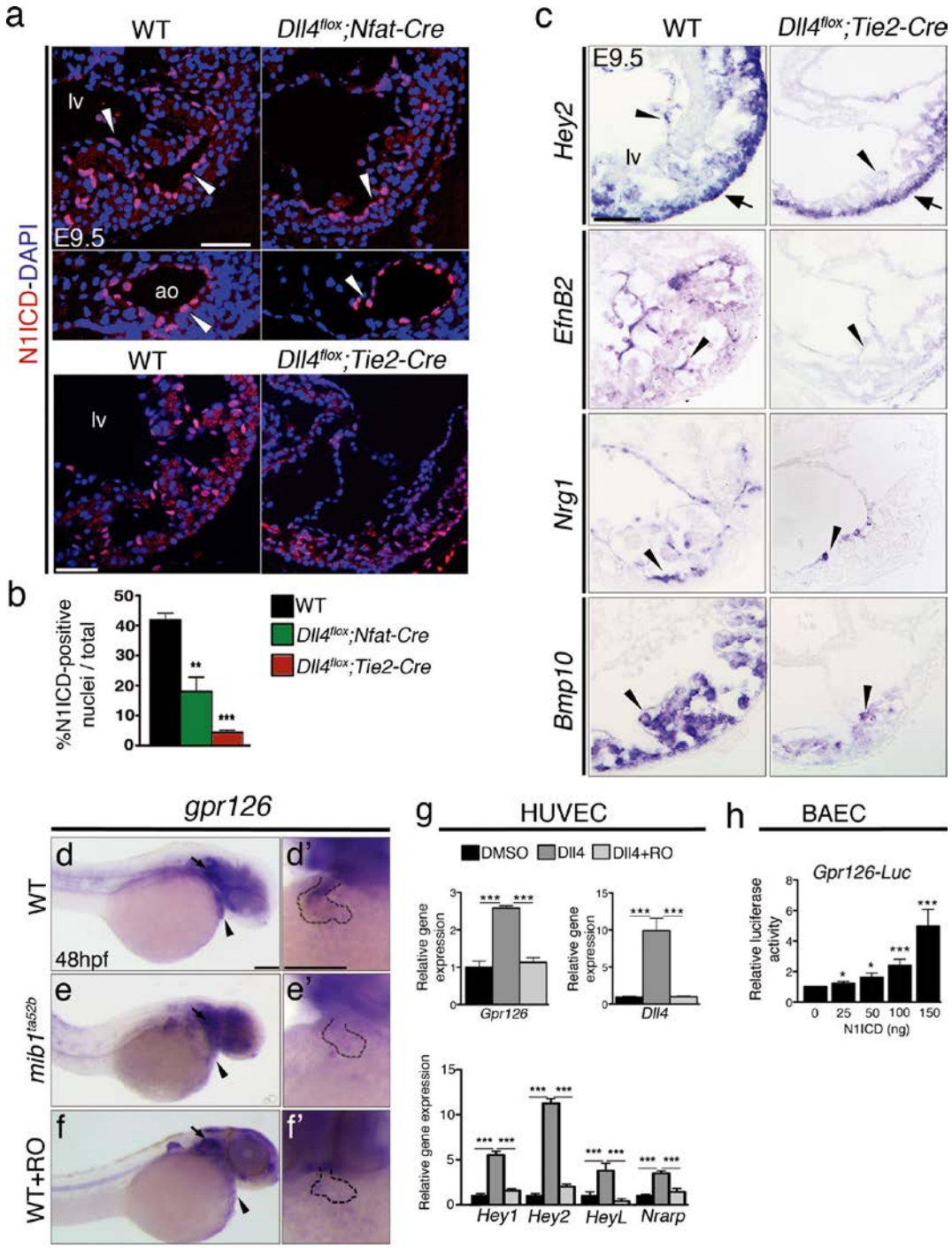

Supplementary Figure 2 Dll4 abrogation disrupts Notch activity and trabecular marker expression (**a-c**) and *Gpr126* expression responds to Notch activation (**d-h**). (**a**) *Top*, N1ICD immunostaining in E9.5 WT and *Dll4^{flox};Nfat-Cre* hearts. *Middle*, N1ICD expression in aortic endothelial cells. *Bottom*, N1ICD staining in E9.5 WT and *Dll4^{flox};Tie2-Cre* hearts. (**b**) Ratios of N1ICD-positive to total endocardial nuclei. Data are mean ± S.D. (n=3 WT embryos, n=3 *Dll4^{flox};Nfat-Cre* embryos and *n=3 Dll4^{flox};Tie2-Cre* embryos, $^{**}P<0.01$, $^{***}P<0.001$, by Student's *t* test). (**c**) *Hey2*, *EfnB2*, *Nrg1* and *Bmp10* ISH in E9.5 WT and *Dll4^{flox};Tie2-Cre* embryos. Scale bar=50µm. (**d-f'**) Reduced *gpr126* expression in zebrafish larvae with impaired Notch signalling. Panels show lateral and ventral views. Lateral and ventral views of the ISH of *gpr126* in WT (**d,d'**, 27 out of 29; 93%), *mib1^{ta52b}* mutant (**e,e'**, 35 out of 38; 92%) and RO-treated WT (**f,f'**, 19 out of 22; 86%), 48-h.p.f. zebrafish embryos showing *gpr126* transcripts in the heart tube (arrowhead) and ear region (arrow) in **d**, and reduced expression in **e,f**. Scale bar=50µm. (**g**) qRT-PCR analysis showing the effect of Dll4- or Dll4+RO-stimulation on the transcription of *Gpr126*, *Dll4* and the Notch targets *Hey1*, *Hey2*, *HeyL* and *Nrarp* in HUVEC. Data are mean ± S.D. (n=4 independent biological replicates for each condition; * $P<0.05$, ** $P<0.01$, *** $P<0.001$ by Student's *t* test). (**h**) *Gpr126* reporter activity measured by luciferase assay in BAEC. Data are mean ± S.D. (n=4 independent biological replicates for each condition; ** $P<0.01$, *** $P<0.001$ by Student's *t* test). Source data available in Supplementary Table 4.

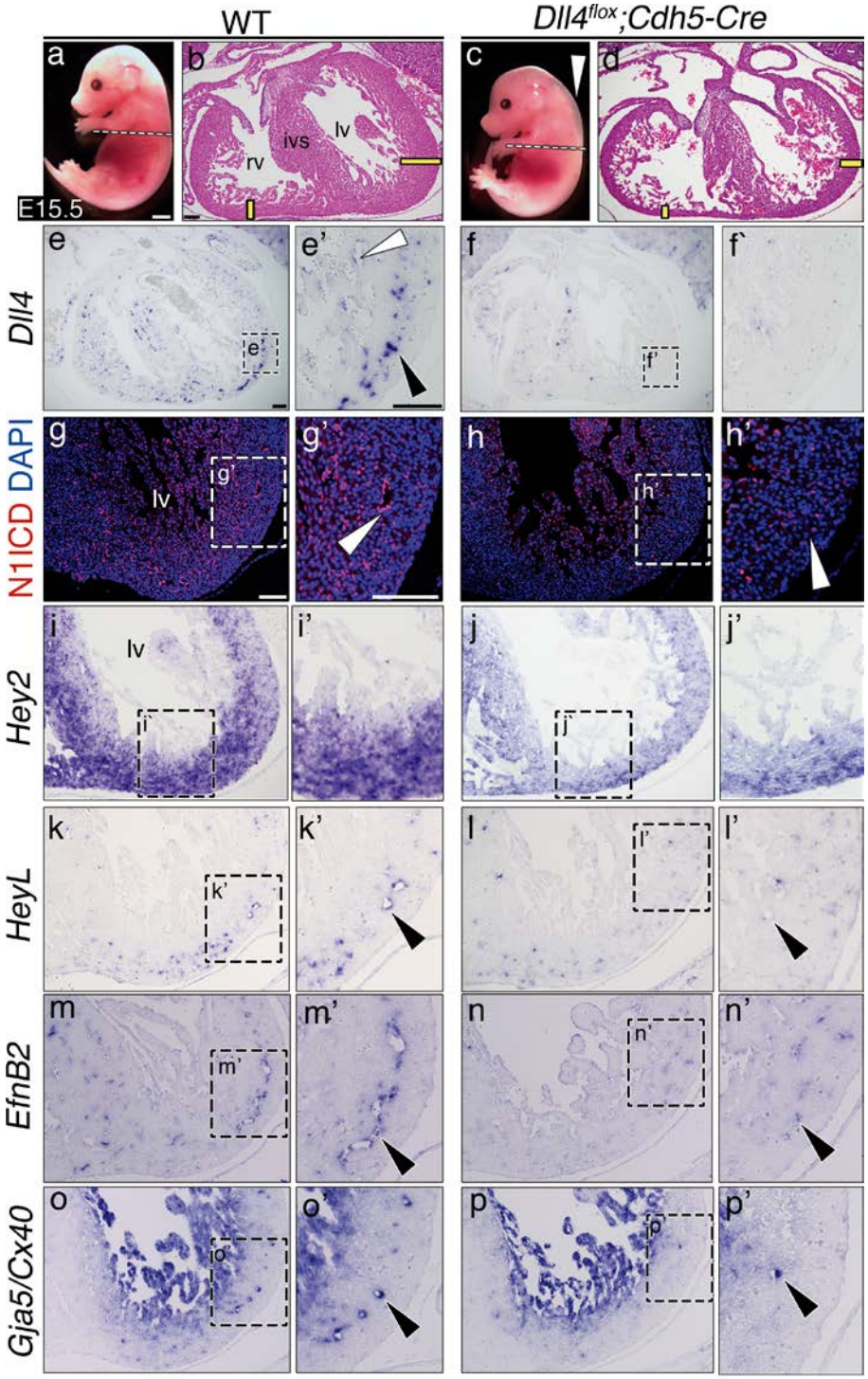

Supplementary Figure 3 Dll4-Notch1 activity is required for coronary vessel formation. (**a,c**) Images of whole-mount E15.5 WT and *Dll4*$^{flo/floxx}$*;Cdh5-Cre/+* (*Dll4*^{flox}*;Cdh5-Cre*) mutant embryos. Note the dorsal oedema (arrowhead) in the mutant embryos. Scale bar=2mm. Dotted lines indicate the plane of the H&E stained sections shown in (**b,d**). The heart in the *Dll4*^{flox}*;Cdh5-Cre* mutant has thinner ventricular walls (**d**, yellow bars) than its WT littermate (**b**). (**e-f'**) ISH in E15.5 hearts. *Dll4* is transcribed in coronary vessel endothelium (**e'**, black arrowhead) and weakly expressed in endocardial cells (**e'**, white arrowhead). Expression is severely impaired in the mutant heart (**f,f'**). (**g-h'**) N1ICD immunostaining. N1ICD staining is strong throughout the endocardium and in coronary vessels of WT ventricle (**g'**, arrowhead), and weak in coronary vessels of mutant embryos (**h'**, arrowhead). (**i-p'**) ISH analysis. (**i-j'**) *Hey2* expression is similar in the compact myocardium of WT embryos (**i,i'**) and mutants (**j,j'**). Note the slightly thinner compact myocardium in the *Dll4*^{flox}*;Cdh5-Cre* mutant heart (**j'**, bracket). (**k-p'**) Expression of the coronary artery endothelial cell markers *HeyL* (**k-l'**), *EfnB2* (**m-n'**) and *Cx40* (**o-p'**) is markedly lower in mutant embryos. The arrowheads mark expression in coronary vessels which appear smaller in *Dll4*^{flox}*;Cdh5-Cre* mutants. Scale bar in (**b,d, e-p'**)=100μm.

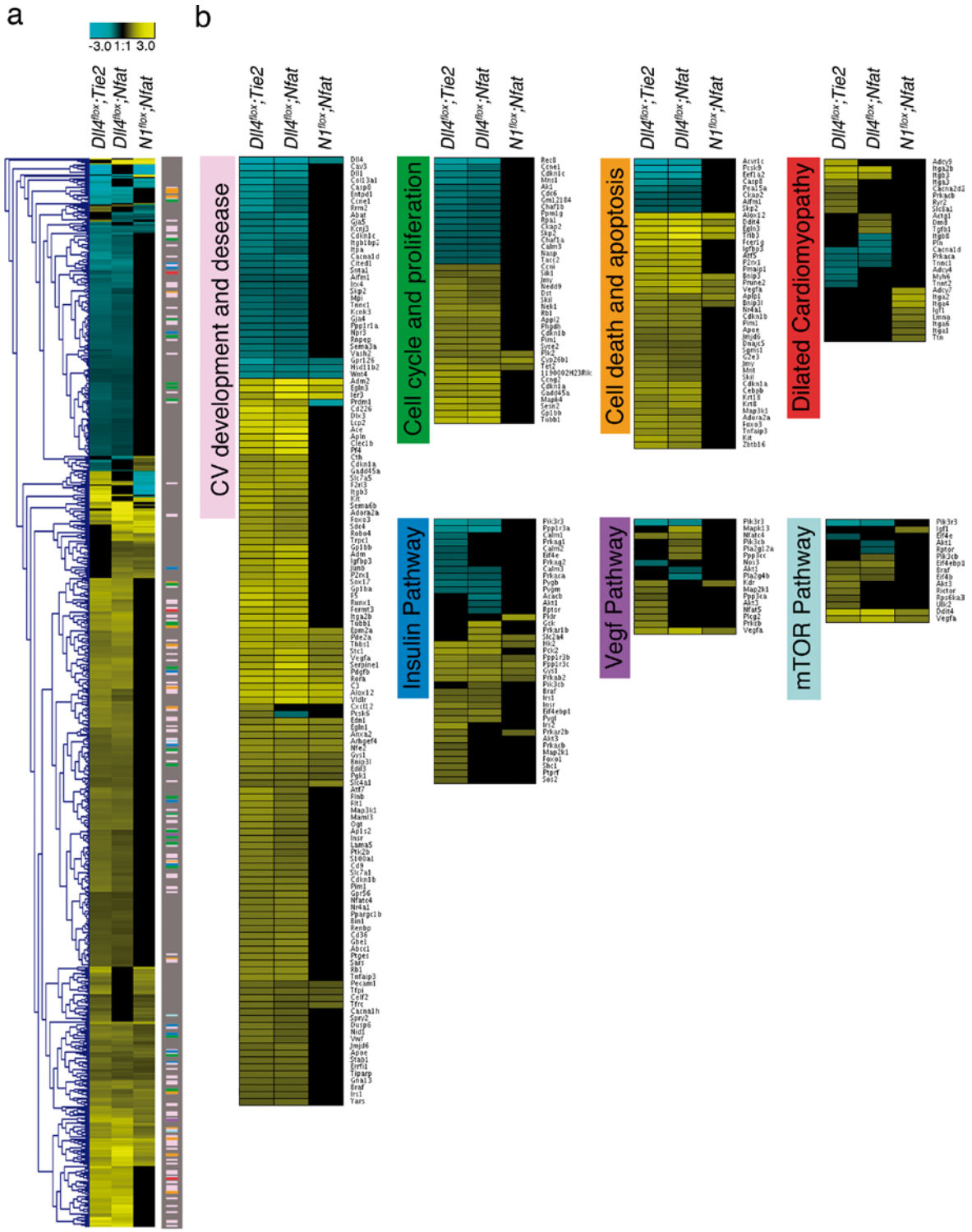

Supplementary Figure 4 Summary of the comparative expression profiling of *Dll4^{flox};Tie2-Cre*, *Dll4^{flox};Nfat-Cre*, and *Notch1^{flox};Nfat-Cre* mutants (**a,b**) and attenuated *gpr126* expression after Notch abrogation in zebrafish (**c-e'**). (**a**) Log fold change (logFC) hierarchical clustering of the 858 genes differentially expressed at E9.5 in the hearts of at least two genotypes among E9.5 *Dll4^{flox};Tie2-Cre, Dll4^{flox};Nfat-Cre* and *Notch1^{flox};Nfat-Cre* mutants. The colour scheme represents the logFC in any of the genotypes compared with its control, with upregulated genes indicated in yellow, downregulated in blue, and black for no significant change. (**b**) Subsets of genes clustered into functional categories (right panels). The total number of deregulated genes for each genotype and the genes represented in the heat map can be found in Supplementary Table 1.

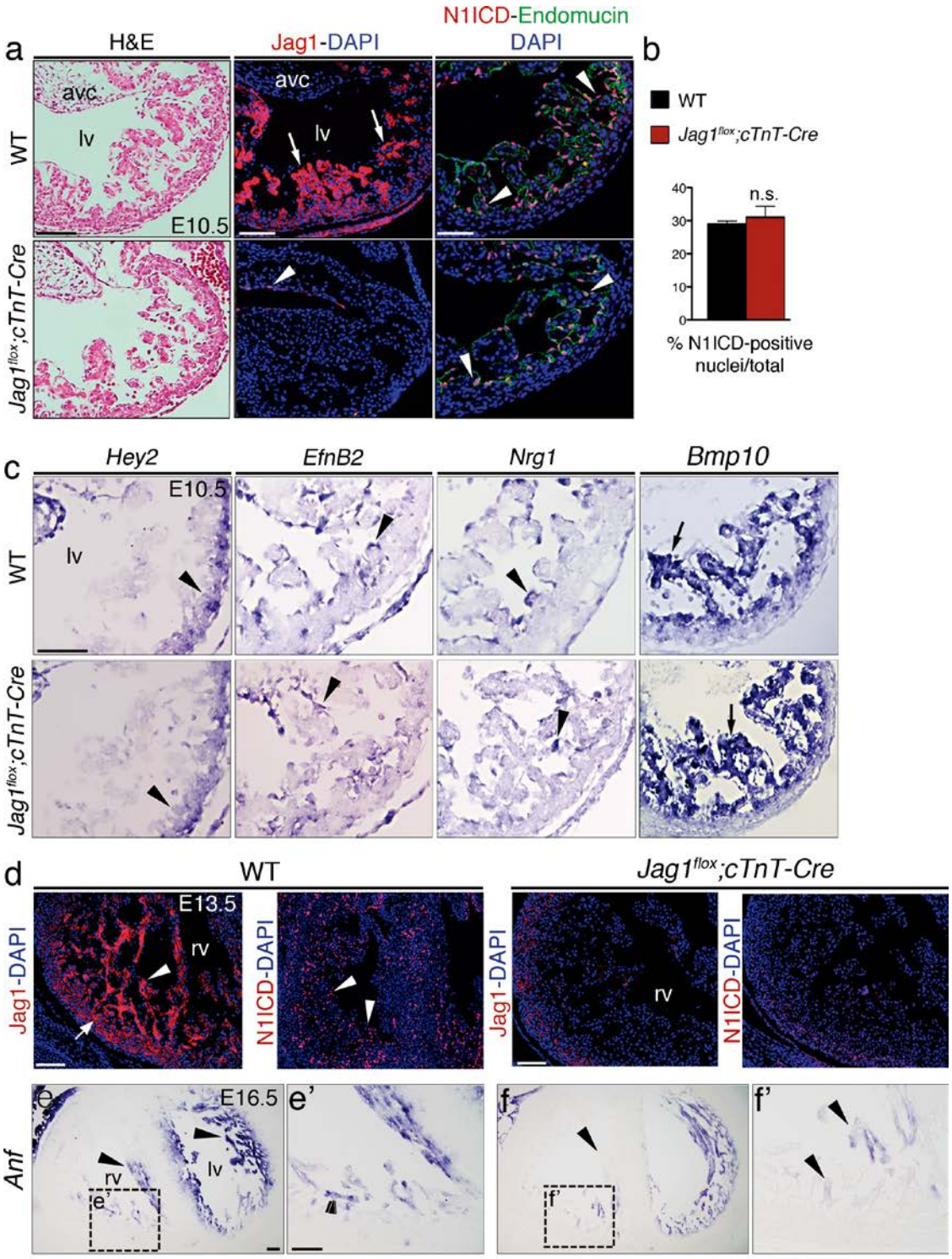

Supplementary Figure 5 Myocardial Jag1 is dispensable for Notch signalling activation during trabeculation (**a-c**) but is required for Notch activation during chamber maturation and compaction and ventricular maturation (**d-f'**). (**a**) E10.5 WT and *Jag1*$^{flox/flox}$*;cTnT-Cre/+* (*Jag1*^{flox}*;cTnT-Cre*) mutant hearts. (**a**) H&E staining. Trabeculae and compact myocardium thickness are similar in WT and mutant hearts. Jag1 (red) is expressed in the trabeculae of the WT ventricle (arrows) but is absent from the mutant ventricle. N1ICD immunostaining (red, arrowheads) in the endomucin-delineated endocardium (green) of WT and *Jag1*^{flox}*;cTnT-Cre* mutant embryos. (**b**) Quantification of N1ICD-positive nuclei as the mean percentage of total nuclei in WT and *Jag1*^{flox}*;cTnT-Cre* mutant embryos. Data are mean ± S.D. (n=3 WT and n=3 mutant embryos, n.s., not significant, by Student's *t* test). (**c**) ISH. *Hey2, EfnB2, Nrg1* and *Bmp10* are normally expressed in E10.5 mutant hearts. (**d**) E13.5. Jag1 and N1ICD immunostainings in WT (**d**, left) and *Jag1*^{flox}*;cTnT-Cre* mutant heart sections (**d**, right). Jag1 is strongly expressed in trabecular myocardium (arrowhead) and weakly in compact myocardium (arrow). N1ICD is expressed throughout the endocardium (arrowheads). Myocardial deletion of *Jag1* attenuates Notch1 activity. (**e-f'**) *Anf* ISH. E16.5 WT heart showing normal expression in trabeculae and septum (**e,e'**, arrowheads) and reduced expression in *Jag1*^{flox}*;cTnT-Cre* hearts (**f,f'**, arrowheads). Abbreviations as in previous figures. Scale bar=100μm. Source data available in Supplementary Table 4.

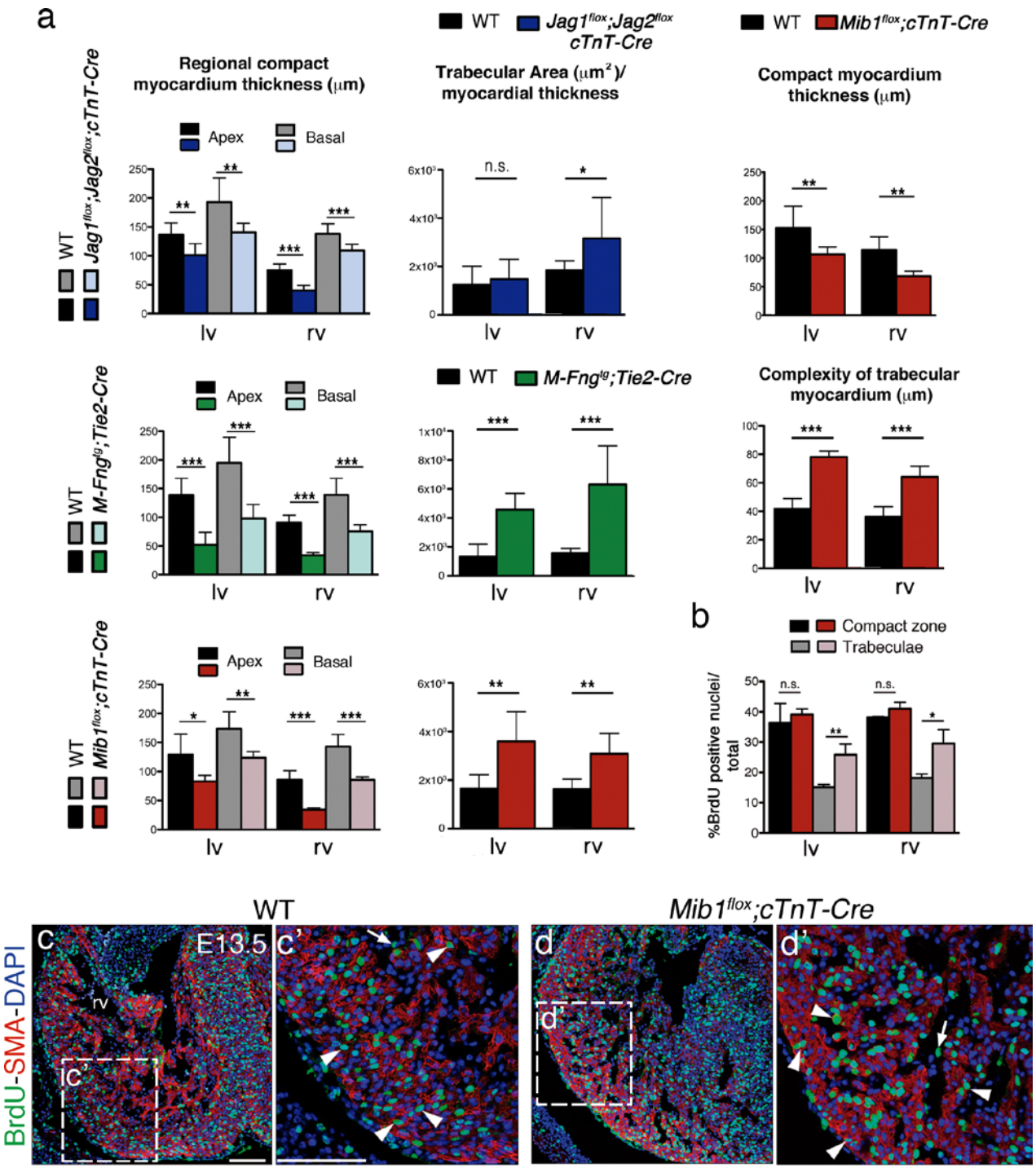

Supplementary Figure 6 Quantification of regional compact myocardium thickness and trabecular area in E16.5 *Jag1^{flox};Jag2^{flox};cTnT-Cre*, *M-Fng^{tg};Tie2-Cre* and *Mib1^{flox};cTnT-Cre* mutants (**a**), compact myocardium thickness and complexity of trabecular myocardium in E16.5 *Mib1^{flox};cTnT-Cre* mutants (**a**) and cellular proliferation in E13.5 *Mib1^{flox};cTnT-Cre* mice (**b,c-d'**). (**a**) For quantification of the morphological parameters the following number of samples were analysed per genotype: *Jag1^{flox};Jag2^{flox};cTnT-Cre* (n=3 WT and n=3 mutant embryos), *M-Fng^{tg};Tie2-Cre* (n=3 WT and n=4 mutant embryos) and *Mib1^{flox};cTnT-Cre* (n=3 WT and n=3 mutant embryos). (**b,c-d'**) Cellular proliferation measured by BrdU immunostaining. BrdU (green), SMA (red) and DAPI (blue) staining of E13.5 WT (**c,c'**) and *Mib1^{flox};cTnT-Cre* heart (**d,d'**). The arrows point to BrdU-positive endocardial nuclei and the arrowheads to BrdU-positive cardiomyocytes. Scale bar=100μm. Data are means ± S.D. (**P*<0.05, ***P*<0.01, ****P*<0.001, by Student's *t* test. n.s., not significant). Source data available in Supplementary Table 4.

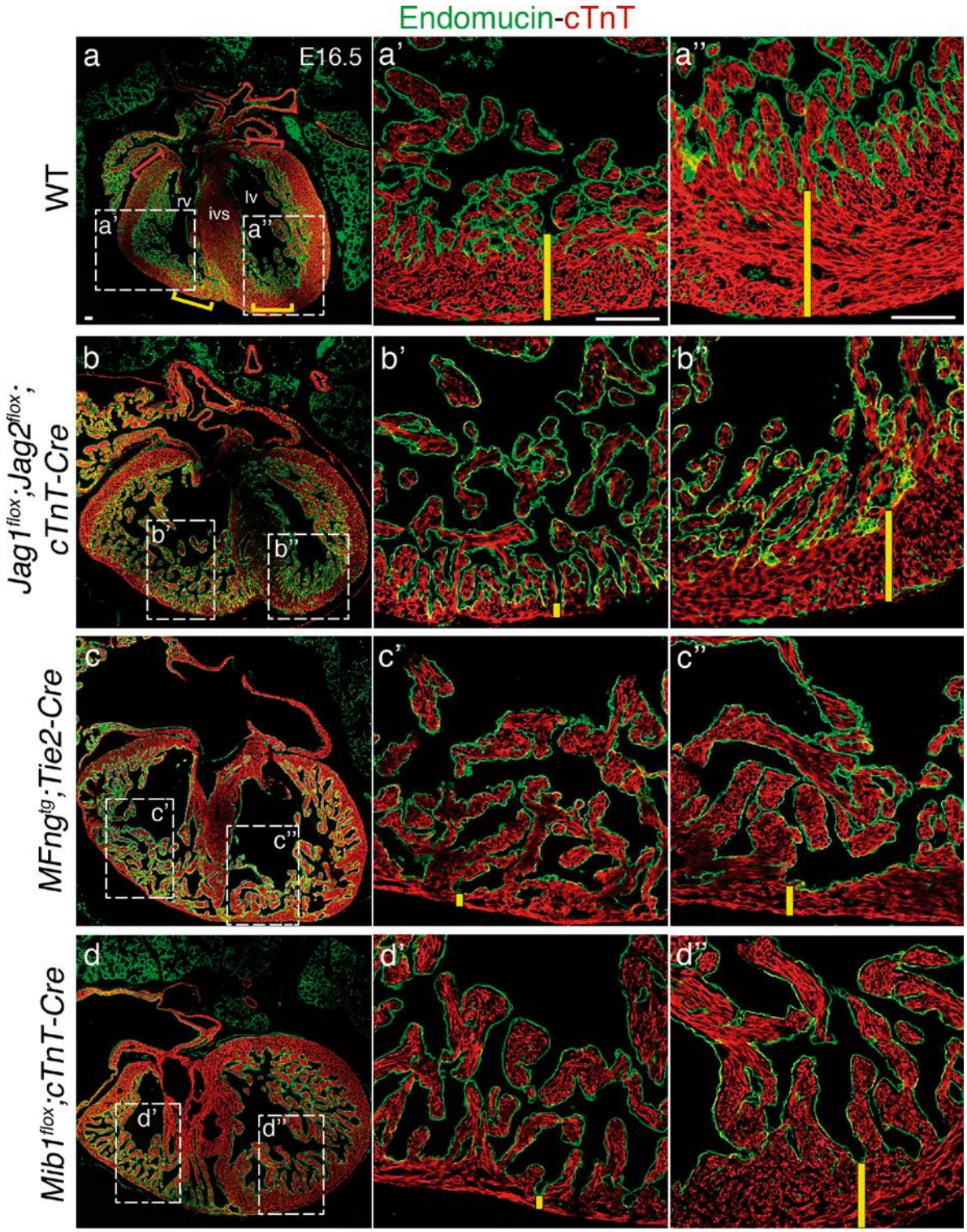

Supplementary Figure 7 Notch signalling abrogation disrupts compaction. E16.5 heart sections stained with endomucin (green) and cTnT antibodies (red) to delineate chamber endocardium and myocardium. The WT heart (**a-a"**) has a thick, cTnT-positive compact myocardium in both ventricles, with compacting trabeculae covered by endomucin-positive endocardium. The *Jag1^{flox};Jag2^{flox};cTnT-Cre* (**b-b"**), *M-Fng^{tg};Tie2-Cre* (**c-c"**) and *Mib1^{flox};cTnT-Cre* hearts (**d-d'**) show very thin compact myocardium, uncompacted trabeculae and disrupted ventricular septum. The white bars in (**a'-d"**) indicate compact myocardium thickness. The red and yellow brackets in (**a**) indicate the basal and apical regions measured to determine the compact myocardium thickness shown in Fig. 2,4,5 and 6. The yellow bar indicates the thickness of compact myocardium. Scale bar=100μm.

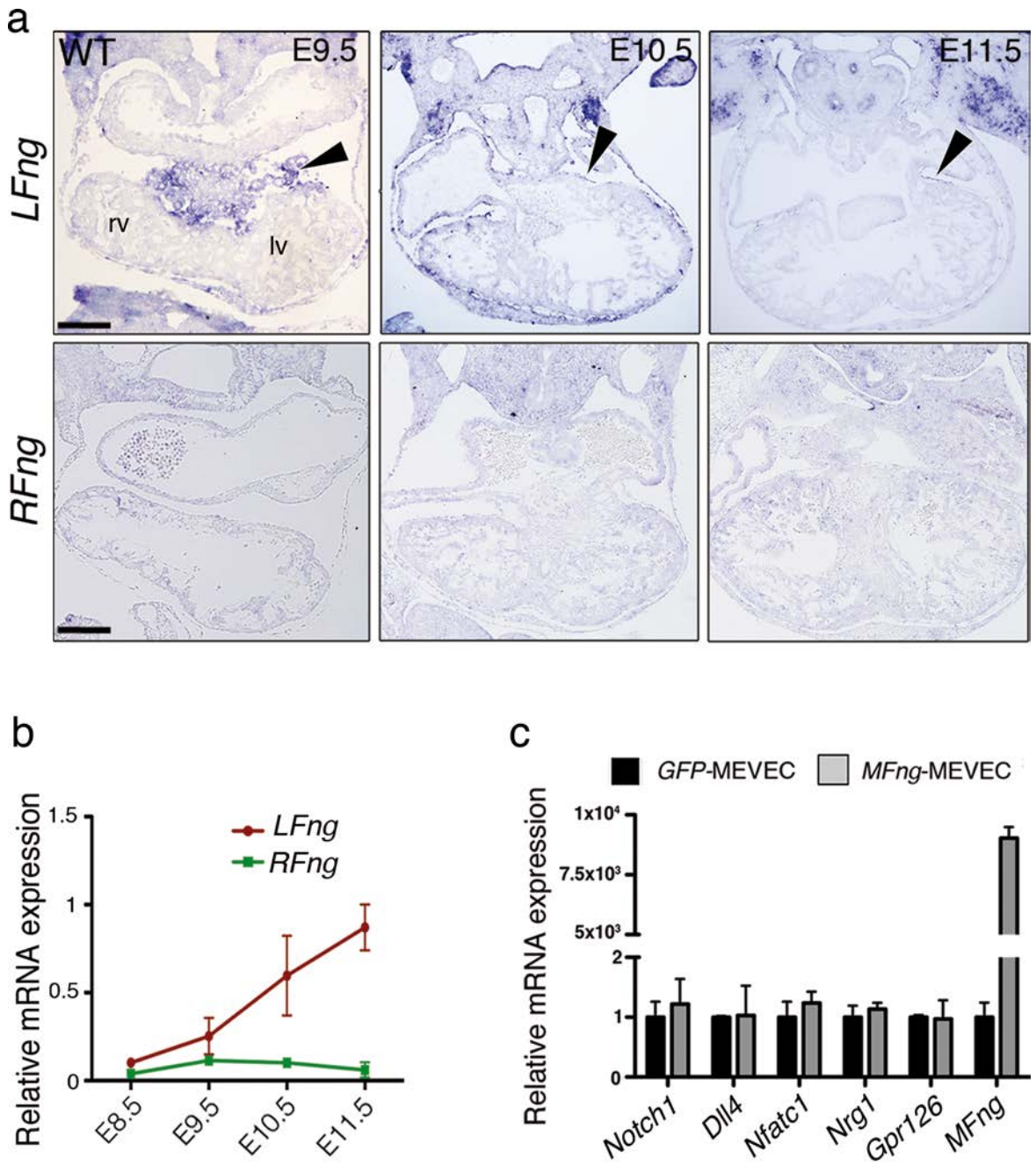

Supplementary Figure 8 Analysis of *Lunatic Fringe* and *Radical Fringe* expression in the embryonic heart (**a,b**) and characterization of gene expression in *GFP*-MEVEC and *MFng*-MEVEC (**c**). (**a**) ISH analysis of *LFng* and *RFng* in WT hearts. *LFng* expression is detected in proepicardial cells of E9.5 embryos (arrowhead) and is restricted to the epicardium of E10.5 and E11.5 hearts (arrowheads). *RFng* is not detected in the heart at these stages. (**b**) Relative mRNA expression of *LFng* and *R-Fng* in E.8.5-E11.5 ventricles. Data are means ± S.D. (n=3 pools of 5 WT hearts at E8.5, and n=3 pools of 3 ventricles per pool at E9.5-E11.5. (**c**) MEVEC. qRT-PCR analysis of Notch pathway genes and endocardial markers, indicating similar expression levels of these genes in *GFP*-MEVEC and *MFng*-MEVEC. Note the very high *MFng* transcript expression after lentiviral transduction in MEVEC. Data are means ± S.D. (n= 2 independent biological replicates for each condition). Scale bar=100μm. Source data available in Supplementary Table 4.

Supplementary Video Legends

Supplementary Video 1. Imaris 3D reconstruction of whole-mount stained E9.5 *CBF1:2HB-Venus* heart. The myocardial surface in red was built from the SMA staining. Venus (white nuclei), revealing Notch activity in CD31/Pecam1-positive cells (green), can be observed in the ventricular endocardium. Nuclei are counterstained with DAPI.
Supplementary Video 2. Representative Z-stack of CMRI short axis views of hearts from 6-month-old WT and *Jag1^{flox};cTnT-Cre* mice. The mutant heart exhibits dilated ventricles and a thinner septum than the WT heart.
Supplementary Video 3 Representative M-mode echocardiography analysis of the hearts of 6-month-old WT and *Jag1^{flox};cTnT-Cre* mice. The mutant heart shows contraction defects.
Supplementary Video 4. Representative Z-stack of CMRI short axis views of hearts from 6-month-old WT and *Jag1^{flox};cTnT-Cre* mice. The mutant heart exhibits a remarked segmental dyskinesia in the RV free wall.

Supplementary Data File Legends

Supplementary Data File 1. AMIRA 3D reconstruction of Dll4 expression (red) at E9.5. The myocardial surface (SMA-positive) is shown in green and DAPI-stained nuclei in blue. The reader can rotate, zoom or crop the model. The buttons on the left allow modification of the different layers. The 3D-view reveals stronger expression of Dll4 in the endocardium at the base of the developing trabeculae.
Supplementary Data File 2. AMIRA 3D reconstruction of Jag1expression at E9.5. Colours reflect myocardial Jag1 expression levels, with red indicating strong expression and blue no expression (as in the compact myocardium). The 3D-view reveals strong Jag1 expression in the outflow tract and atrial myocardium. Moderate Jag1 expression is observed in the trabecular myocardium.
Supplementary Data File 3. AMIRA 3D reconstruction of NICD (red) at E9.5. The myocardial surface (SMA-positive) is shown in green and DAPI stained nuclei in blue. The 3D-view reveals strong N1ICD expression at the base of the developing trabeculae.

Supplementary Table Legends

Supplementary Table 1. Excell file containing the list of deregulated genes identified by RNA-seq analysis (upregulated genes in red and downregulated genes in green). E9.5 *Dll4^{flox};Tie2-Cre* (sheet 1); E9.5 *Dll4^{flox};Nfat-Cre* (sheet 2); E9.5 *Notch1^{flox};Nfat-Cre* (sheet 3). 144 common deregulated genes from E9.5 *Dll4^{flox};Tie2-Cre, Dll4^{flox};Nfat-Cre* and *Notch1^{flox};Nfat-Cre* listed by the log fold change (logFC) of the *Dll4^{flox};Tie2-Cre* (sheet 4, related to Fig. 1k). E15.5 *Jag1^{flox};cTnT–Cre* (sheet 5); E15.5 *Jag2^{flox};cTnT–Cre* (sheet 6); E15.5 *Jag1^{flox};Jag2flox;cTnT–Cre* (sheet 7); E15.5 *MFng^{GOF};Tie2–Cre* (sheet 8). Combined analysis of E15.5 *Jag1^{flox};cTnT–Cre, Jag2^{flox};cTnT–Cre* and *Jag1^{flox};Jag2flox;cTnT–Cre* with batch correction; deregulated genes are organized according to the logFC of the *Jag1^{flox};Jag2flox;cTnT–Cre* (sheet 9). E14.5 *Mib^{flox};cTnT-Cre* RNASeq from [15] re-analysed using GRCm38 genebuild (sheet 10). Genes represented in the circular plot of *Dll4^{flox}* and *Notch1^{flox}* mutants (sheet 11, related to Fig. 1l); genes represented in the circular plot of *Jag1^{flox};cTnT –Cre* mutants (sheet 12, related to Fig. 3b); logFC of the 319 genes shown in the heat map of Figure 7c (sheet 13).

Supplementary Table 2. Excell file containing the list of primary and secondary antibodies used in this study to immunodetect proteins in whole-mount or paraffin sections.

Supplementary Table 3. Excell file containing the qPCR primers used in this study.

Supplementary Table 4. Excell file containing the statistics data source

Dll4 Expression Pattern at E9.5

Layers

Nuclei

Dll4

Myocardium

Views

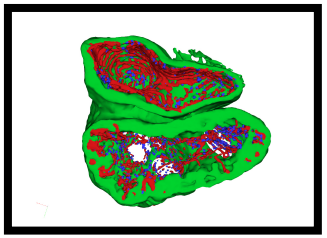

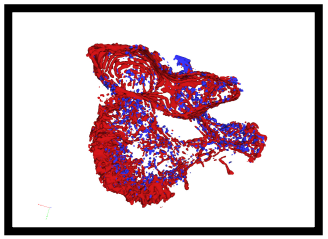

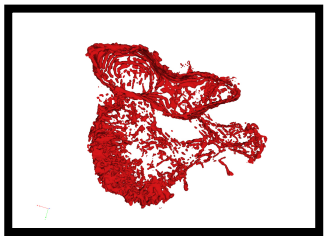

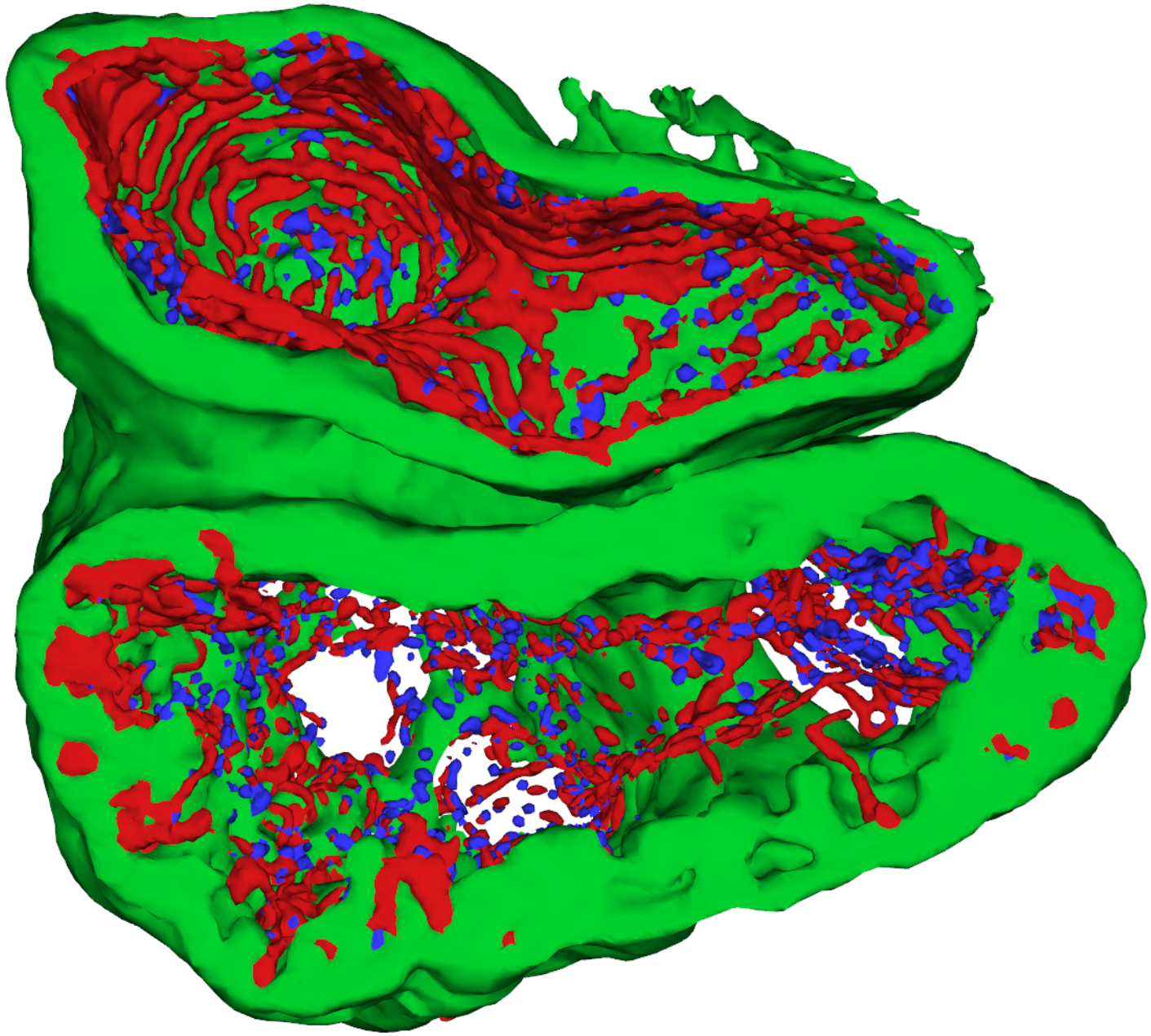

Dll4 Expression Pattern at E9.5

Layers

- AVC
- Compact Myocardium
- Trabecular Myocardium
- Atrium
- Outflow Tract

Views

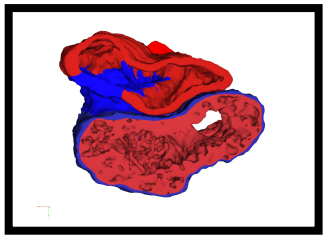

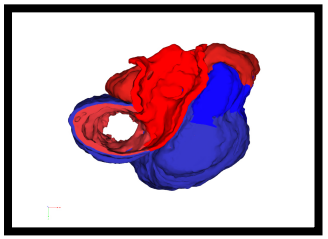

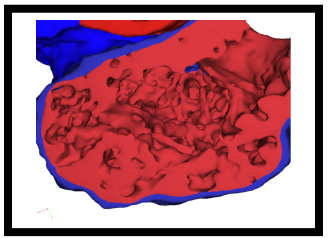

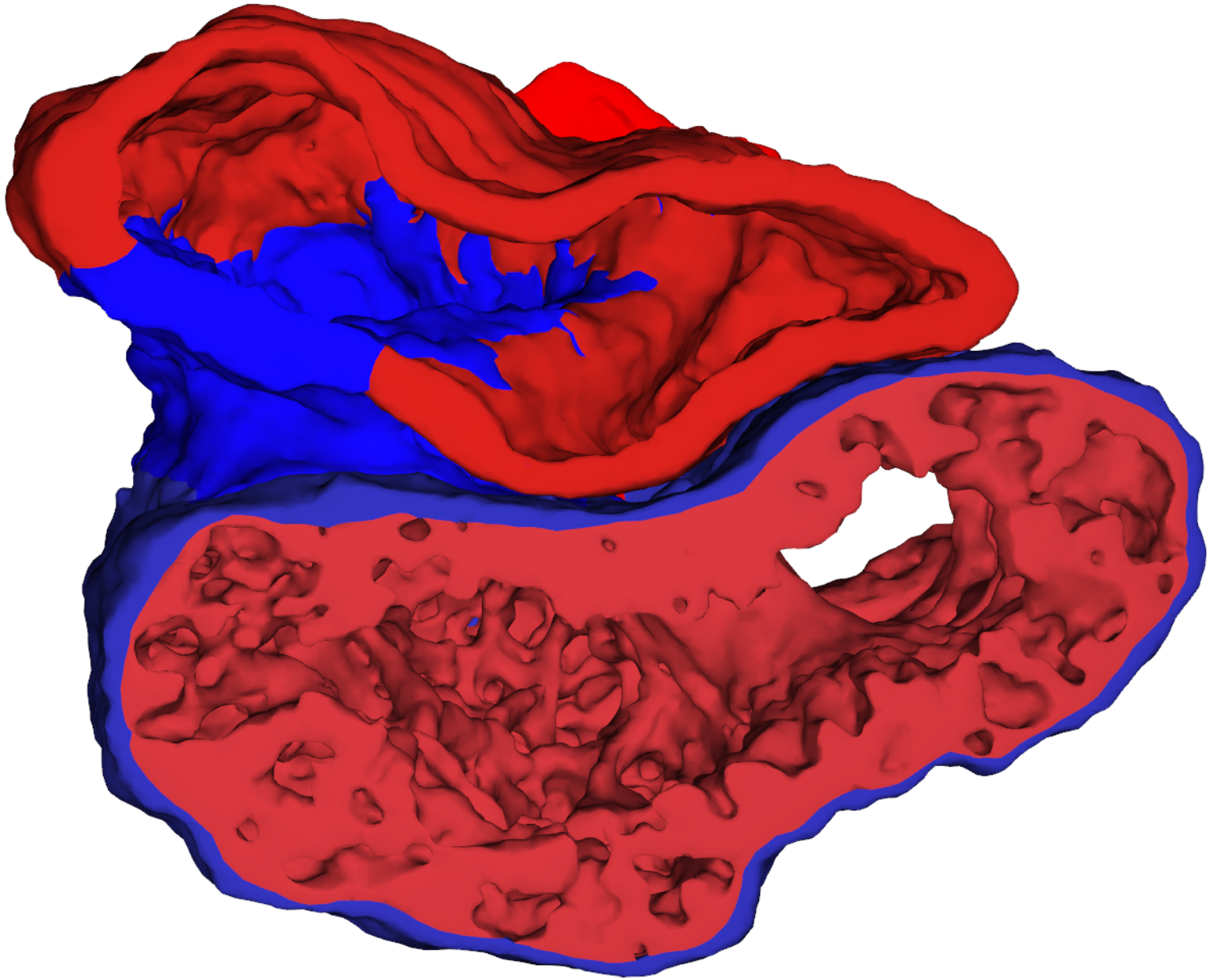

Dll4 Expression Pattern at E9.5

Layers

Nuclei

N1ICD

Myocardium

Views